JOURNAL OF MATERIALS SCIENCE 30 (1995) 6267–6272

Experimental investigation of the transformation zone of tetragonal zirconia polycrystalline ceramics

QING XINLIN*, QIN YUWEN
Department of Mechanics, Tianjin University, Tianjin 300072, People's Republic of China
DAI FULONG, SUN QINGPING
Department of Engineering Mechanics, Tsinghua University, Beijing 100084, People's Republic of China

Stress-induced martensitic transformation plastic zones of ceria-stabilized tetragonal zirconia polycrystalline ceramics, under some typical loading conditions, were studied by Moiré interferometry. The full-field fringe patterns, including *u*-fields and *v*-fields, were acquired. According to these patterns, the transformation zone shape and transformation plasticity distributions of the specimens were obtained. The experimental results show that the stress-induced transformation at room temperature is concentrated in some narrow bands and the transformation plasticity is not uniform within the transformation zone. Experiments also reveal that the transformation zone with a characteristic elongated shape ahead of the notch, in a single-edge notch bending specimen, is obviously different from that resulting from some constitutive relation of transformation. This work provides a significant experimental foundation for establishing the theoretical models of transformation toughening.

1. Introduction

The transformation zone formed in the stress field of crack tips in transformation-toughened ceramics plays an essential role in the crack-shielding mechanism of toughening [1–4]. The amount of toughness enhancement principally depends on the shape and the detailed transformation plasticity strain distribution within the zone. The transformation zones have been detected by several techniques [5–12]: X-ray diffraction, transmission electron microscopy, Raman spectroscopy and observations by optical interference methods of surface distortions due to the transformation strain. However, these methods have not yet been used to provide a sufficiently quantitative measurement of the distribution of transformation plasticity. Detailed knowledge of transformation plasticity, especially of its constitutive behaviour, is essential for an understanding of transformation toughening. It is clear that there exist two important ways to achieve the aim. One is to perform direct measurements of transformation strains within the crack tip zone by some techniques. The other way is to perform the plastic strain-field measurement of the material under a simple stress state such as tension, which, from the point of view of constitutive research, is very important because not only is the material in the mode I crack tip region mainly subjected to tension, but also such a simple stress state can reveal some important deformation features of this material during transformation. So far, even though many research works on transformation plasticity zone have been performed, it is far from sufficient.

Moiré interferometry is a high sensitivity, high spatial resolution, full-field optical method of measurements of in-plane displacements on the surface of a specimen [13]. It can be suited to micromechanics study of material to a certain degree. Some significant applications of Moiré interferometry have been made in recent years [14].

In this work, the transformation zone shape and the transformation plasticity distribution within the zone were studied by Moiré interferometry. Some new phenomena were discovered and are discussed.

2. Experimental procedure

2.1. Specimens

The test material was a ceria-stabilized tetragonal zirconia polycrystal (Ce-TZP). The ZrO_2 powder containing 10 mol % CeO_2, prepared by a coprecipitation technique, was isostatically pressed at 250 MPa and then sintered at 1350°C for 2 h in air. The as-sintered compacts were ground to a flat "dog-bone" tension specimen, and a beam and bending specimen with single-edge notch, respectively, and the surfaces were polished with diamond paste from 20 μm to 1 μm followed by annealing at 1200 °C for 20 min. The sizes and the loading conditions of the above three kinds of

**Present address*: Department of Engineering Mechanics, Tsinghua University, Beijing 100084, P.R. China.

0022–2461

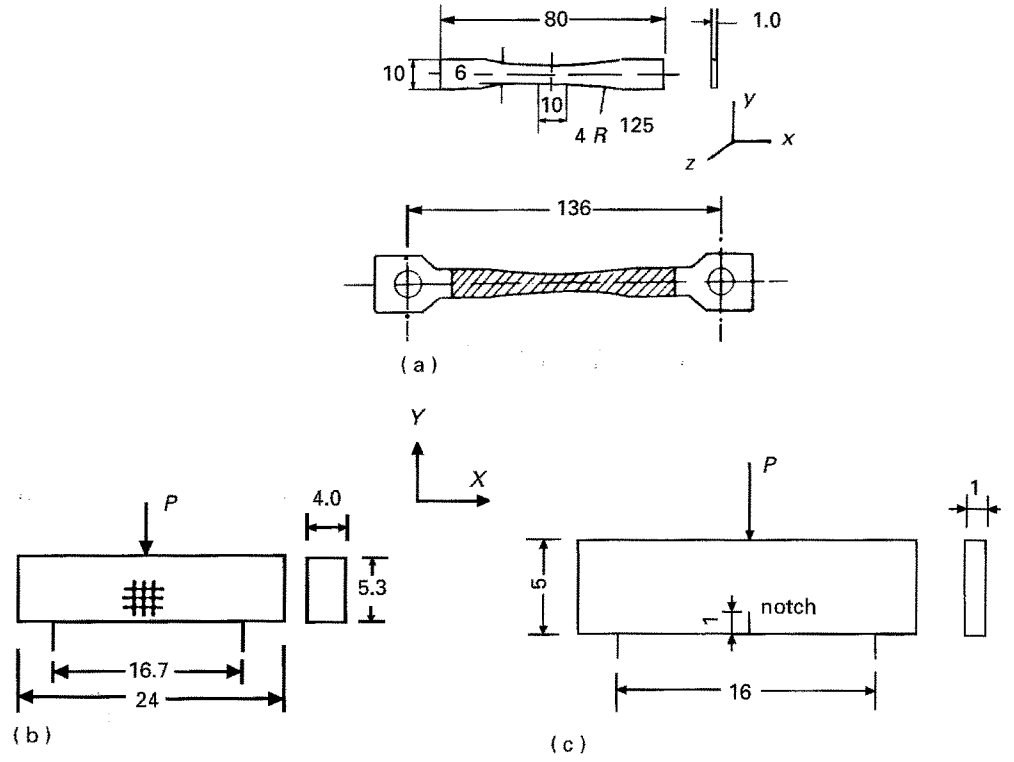

Figure 1 The sizes and loading conditions of (a) the tensile specimen, (b) the three-point bending beam, and (c) the beam with a single-edge notch for Ce-TZP. Dimensions in millimetres.

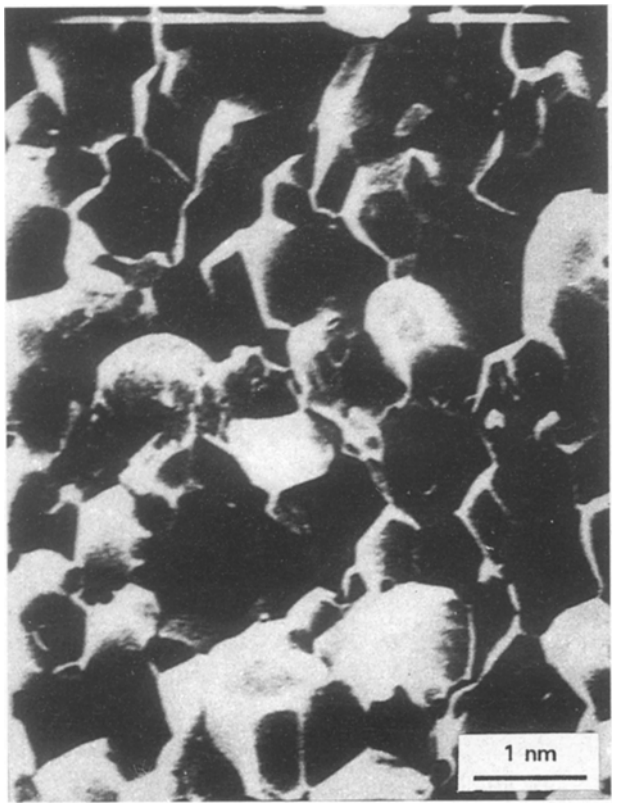

Figure 2 Scanning electron micrograph of a section for Ce-TZP.

specimen are shown in Fig. 1. A scanning electron micrograph of a section of the specimens is shown in Fig. 2. A crossed-line diffraction grating, which has a frequency of 1200 1/mm, was replicated on the surface of each specimen. In the uniaxial tension specimen, two strain gauges of dimensions 1 mm × 1 mm were also adhered to the tension specimen at the central part on the other surface.

2.2. In-plane displacement measurement

The in-plane displacements were obtained by Moiré interferometry with a sensitivity of 0.417 μm per fringe order. Moiré interferometry is an optical technique which uses the interference of coherent beams to produce contours, or fringe contours, of in-plane surface displacement components (u, v) . The method employs the high-frequency grating which is attached to the surface of the specimen and deforms with the specimen. When the deformed specimen grating is interrogated in an interferometer, fringe patterns corresponding to the u and v displacement fields are obtained. As shown in Fig. 3a, when the two incident beams are symmetrical with respect to the specimen grating and the incident angles of the beams satisfy

$$\theta = \arcsin(\lambda f) \tag{1}$$

where λ is the wavelength of light, f is the frequency of the specimen grating, the displacement components u and v are obtained from the fringe order N_x and N_y by [15]

$$u = \frac{N_x}{2f} \tag{2}$$

$$v = \frac{N_y}{2f} \tag{3}$$

and the in-plane strains by

$$\varepsilon_x = \frac{1}{2f}\frac{\partial N_x}{\partial x} \tag{4}$$

$$\varepsilon_y = \frac{1}{2f}\frac{\partial N_y}{\partial y} \tag{5}$$

$$\varepsilon_{xy} = \frac{1}{2f}\left(\frac{\partial N_x}{\partial y} + \frac{\partial N_y}{\partial x}\right) \tag{6}$$

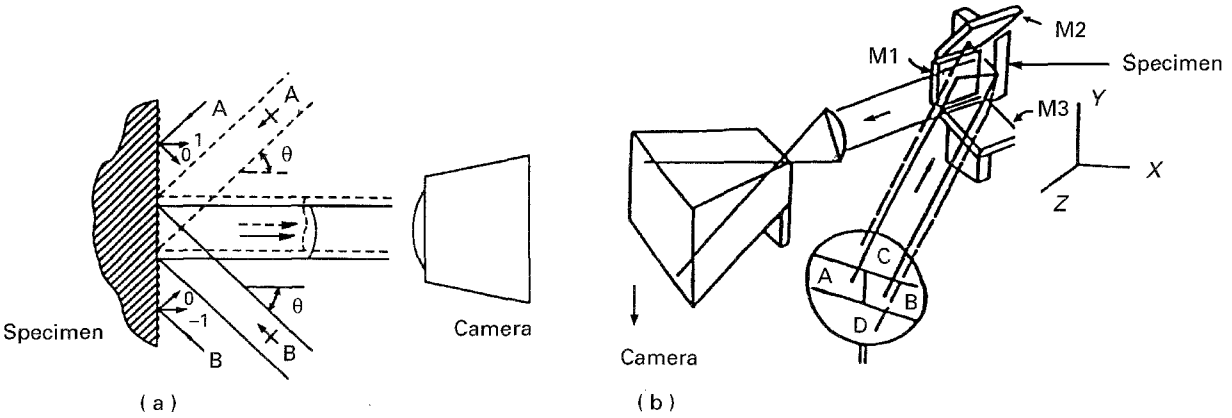

Figure 3 Moiré interferometry apparatus: (a) the basic two-beam system, (b) the three-mirror (M1–M3) optical system.

A three-mirror optical system, as shown in Fig. 3b, was used in the experiment. In the system, a beam selector was used to illuminate the specimen grating with two beams in the horizontal plane. The horizontal component of the displacement field was then recorded photographically. The beam selector was then adjusted to give two beams which, with the aid of the two 45° mirrors in the system, illuminated the specimen grating in the vertical plane. This arrangement provided the vertical component of the displacement field.

The strain gauges, adhered on the surface of the tension specimen, and the X–Y recorder, were used to measure the axial and transverse strains, respectively, in order to keep watch on the deformation of the specimen.

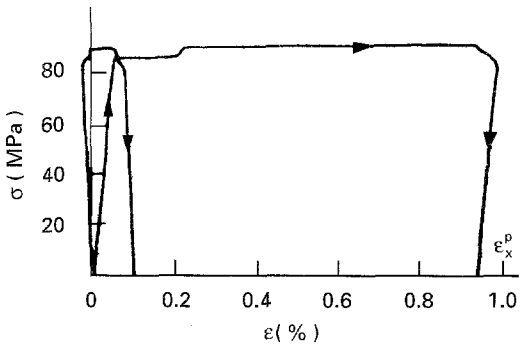

Figure 4 Stress–strain curve in uniaxial tension for Ce-TZP.

3. Results and discussion

3.1. Uniaxial tension experiment

The stress–strain relation curves for tension specimen obtained by the X–Y recorder is shown in Fig. 4. When the applied stress was raised over 85 MPa, the material began to transform from tetragonal to monoclinic phase accompanied by a small load drop and the specimen entered the stage of plastic yielding. The transformation proceeded very quickly so that a noise can be heard during loading. At the initial stage of yielding, two bank-like regions (about 0.1 mm in width) normal to the tensile stress axis were formed in the central equal cross-section part of the specimen, where the Moiré patterns of displacement were more dense than elsewhere. Further loading quickly widened the two bands and joined them into a single one; finally, the transformation zone is formed. The enlarged fringe patterns of the residual deformation within and around the final transformation zone are shown in Fig. 5. Fig. 6(a–c) show the distributions of the residual strains, ε_x^R, ε_y^R, and ε_{xy}^R, within and around the transformation plastic zone. Plastic strain inside the band is not uniform and is much higher than outside. The axial residual strain near the tensile axis is slightly smaller than that at other regions in the transformation zone, and the transverse strain near the axis is much smaller comparatively than that at other points. So the ratio of the axial residual strain to the transversal residual strain at the points on the

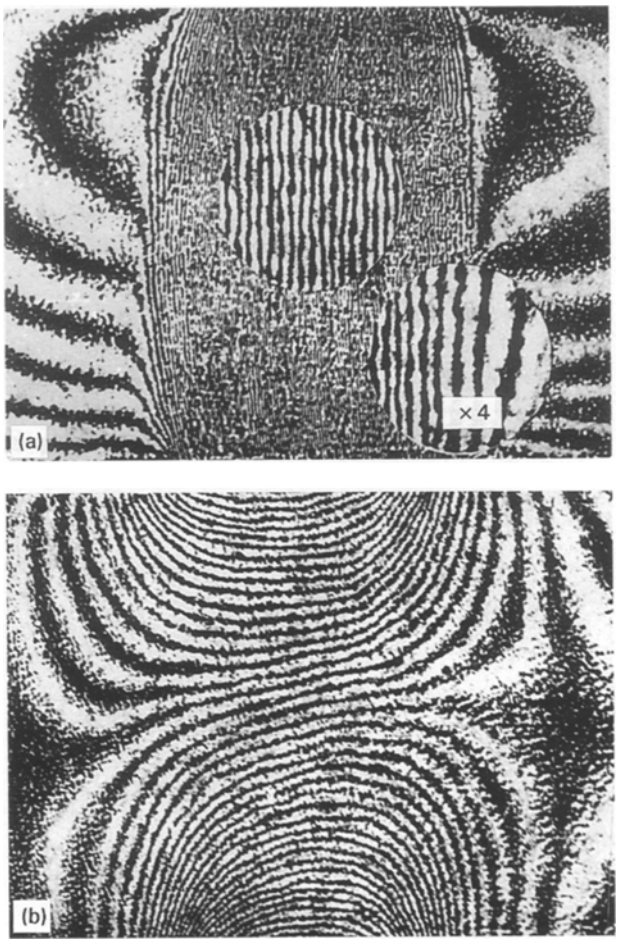

Figure 5 Moiré fringe patterns of residual deformation of the tensile specimen.

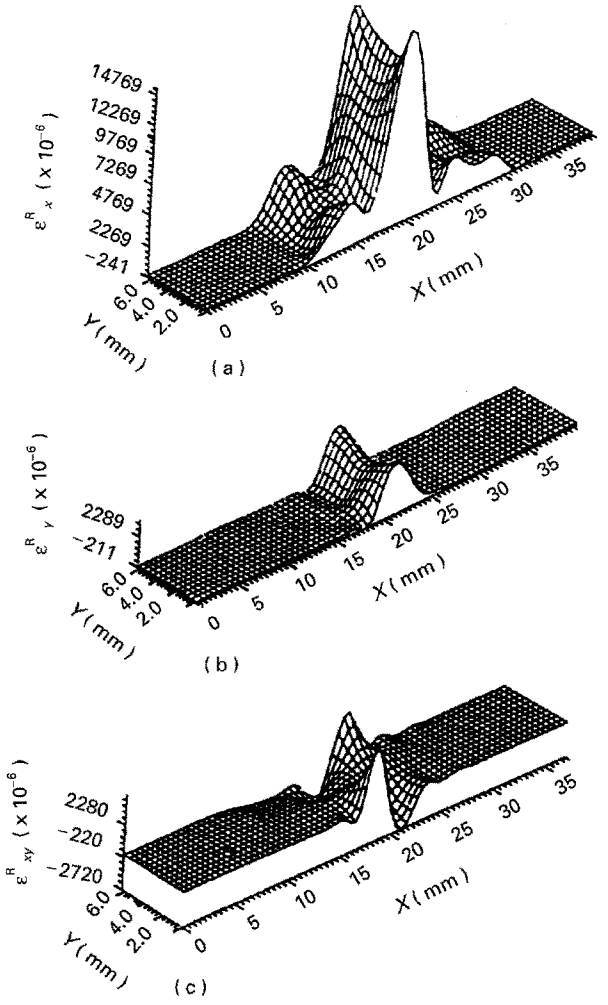

Figure 6 Residual strain distributions of the tensile specimen corresponding to Fig. 5. (a) ε_x^R, (b) ε_y^R, (c) ε_{xy}^R.

region near the central axis is slightly larger than that at other points. The experiment shows once again that the transformation plastic strain is not pure volume dilation and involves a great deviatoric component due to the lattice shear.

3.2. Three-point bending experiment

The Moiré interference fringe patterns for three-point bending beam are shown in Fig. 7. They are u-field and v-field fringe patterns, respectively, at different stages of loading and unloading. Owing to the pressure sensitivity of yielding, the transformation only happens in the tensioned side of the beam and proceeds within a narrow band which is perpendicular to the tensile stress direction. It is clear that instead of a plastic zone, as in metal plasticity, one or more narrow bands where transformation is localized is formed during loading. As a result of asymmetric yielding, the perfect plastic regime of the load–strain curve, as in the uniform tensile experiment, is not observed in bending. The residual axial tensile strain distribution in the side surface is shown in Fig. 8. Similar to uniaxial tension, the axial residual strain is much larger than the transverse residual strain in the transformation band. However, the ratio of axial residual strain to transverse residual strain is larger than that in the transformation zone of the tensile specimen.

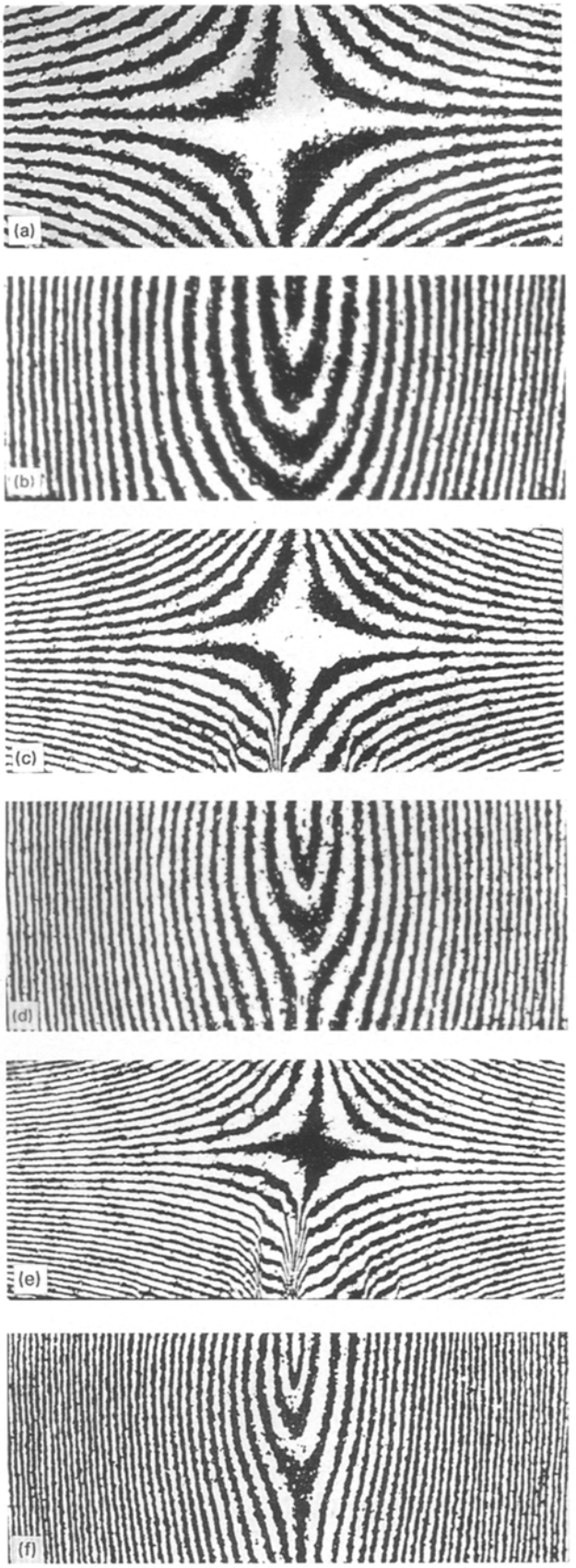

Figure 7 Moiré fringe patterns for the three-point bending beam at different stages of loading: (a, b) 36 N, (c, d) 46 N, (e, f) 58 N, (g, h) unloading; (a, c, e, g) u, (b, d, f, h) v.

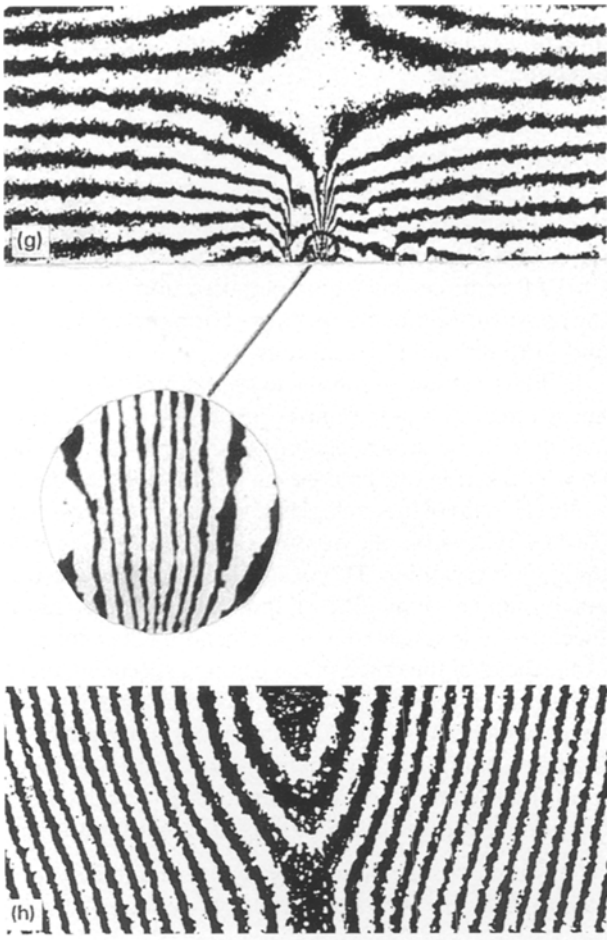

Figure 7 (*Continued*)

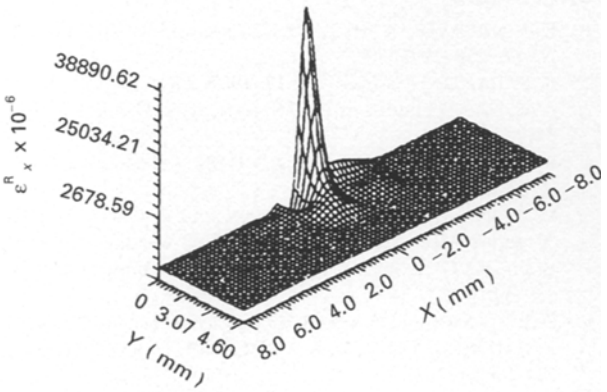

Figure 8 The distribution of the residual strain in the side surface of the beam.

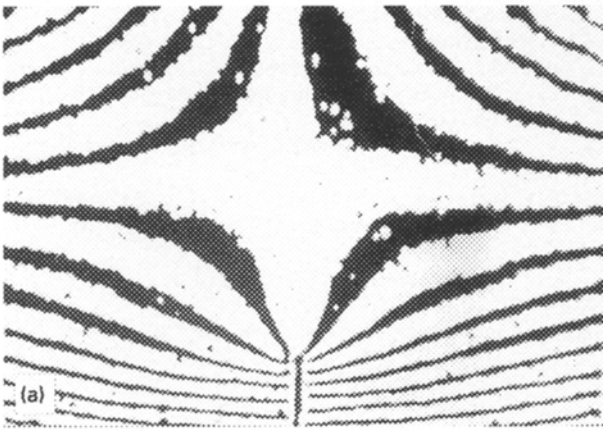

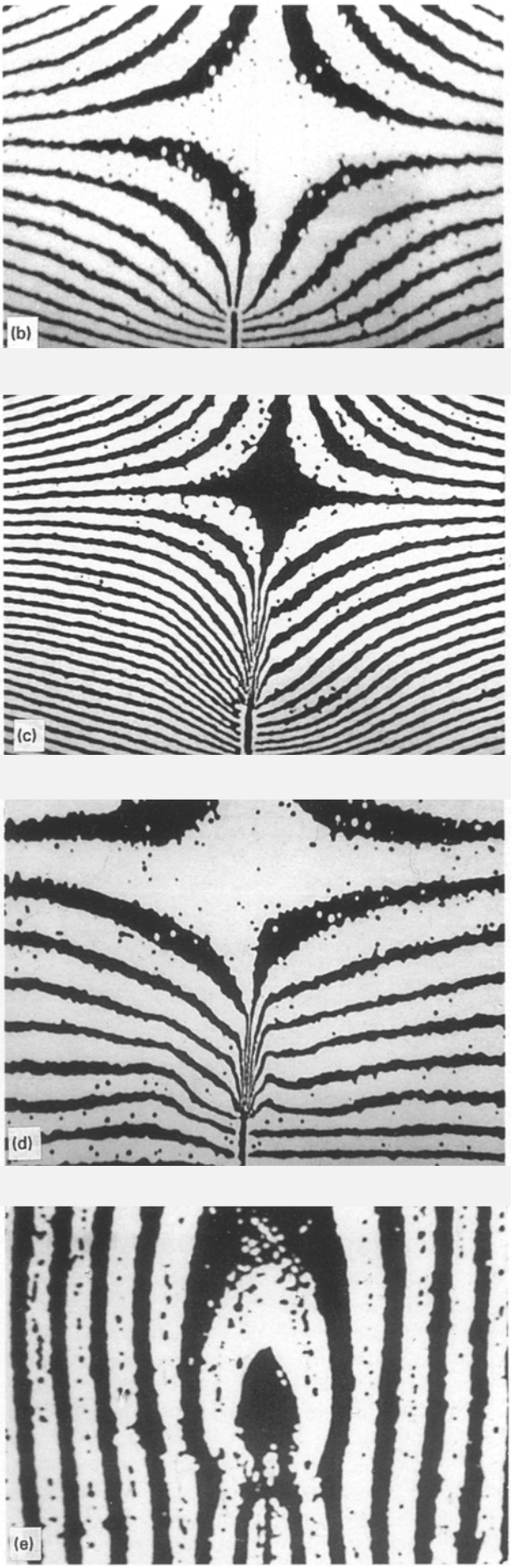

Figure 9 Moiré fringe patterns of the beam with a single-edge notch. (a) $P = 15$ N, u; (b) $P = 20$ N, u; (c) $P = 24$ N, u; (d) unloading, u; (e) unloading, v.

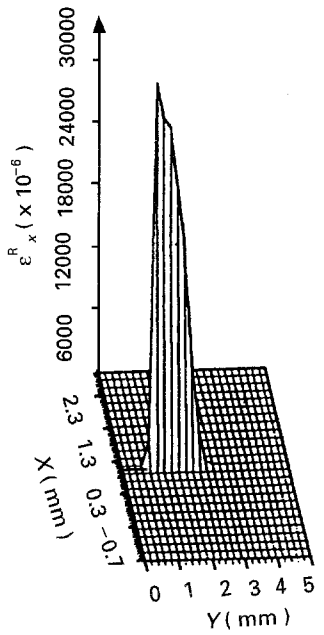

Figure 10 The distribution of the residual strain corresponding to Fig. 9d.

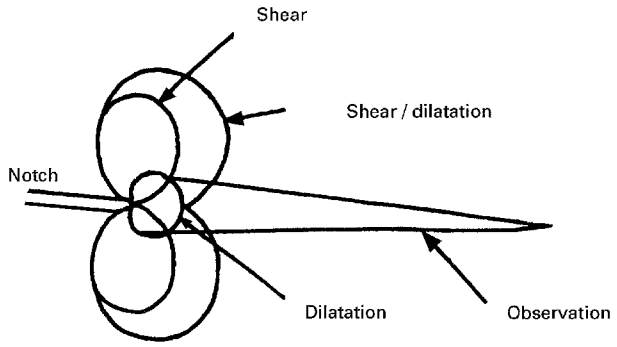

Figure 11 Comparison of the calculated and observed transformation zones.

3.3. The beam with a single-edge notch

The fringe patterns of in-plane displacement in the side surface of the beam with a single-edge notch are shown in Fig. 9. The distribution of residual strain in the tensile stress direction, corresponding to Fig. 9d, is shown in Fig. 10. When the loading, P, approaches 22 N, a narrow region, where the deformation is obviously larger than elsewhere, suddenly appears in front of the notch. The region continually enlarges with increasing load and the strain in the region is also incremental. After loading to P approaching 24 N, a plasticity zone with a characteristic elongated shape ahead of the notch of the specimen is clearly observed. According to the Moiré interferometry fringe patterns at unloading, the shape and size of the transformation zone can be determined, as shown in Fig. 11. Comparing Figs 7d and 9d, it is clear that the transformation zones are concentrated in bands similar to the Dugdale plastic strip zone model [16] and obviously different from the zone shapes resulting from several transformation criteria [10]. In the transformation zone, the strain in the tensile stress direction is far larger than that in the perpendicular direction.

4. Conclusions

1. Under certain thermomechanical loading conditions, the plastic flow localization is one of the most important aspects of transformation plasticity in Ce-TZP ceramics and must be taken into account in the constitutive modelling of transformation plasticity and in toughening calculations.

2. Plastic strain within the deformation bands in the above three kinds of specimen consists of both deviatoric and volumetric strain, demonstrating that the plastic flow localization can proceed via a dilatant shear band.

3. The ratio of the axial plastic strain to the transverse plastic strain within the transformation zone varies with the loading condition. The ratio of the tensile specimen is much smaller than that of the three-point bending specimen and single-edge notch bending specimen.

4. Ahead of the notch of the bending specimen, there is a transformation zone with a characteristic elongated shape, which was similar to the transformation zone of the three-point bending beam and obviously different from the shape of the transformation zone calculated from some constitutive relations of transformation.

The above research work provides valuable experimental data on the constitutive modelling of transformation.

References

1. R. C. GARVIE, R. H. J. HANNINK and R. T. PASCOE, *Nature* **258** (1975) 703.
2. F. F. LANGE, *J. Mater. Sci.* **17** (1982) 247.
3. A. G. EVANS and R. M. CONNON, *Acta Metall.* **34** (1986) 751.
4. P. E. REYES-MOREL and I. W. CHEN, *J. Am. Ceram. Sci.* **72** (1988) 343.
5. M. V. SWAIN, R. H. J. HANNINK and R. C. GARVIE, in "Fracture Mechanics of Ceramics", Vol. 6, edited by R. C. Bradt, A. G. Evans (Plenum Press, New York, 1983) pp. 339–54.
6. D. R. CLARK and F. ADAR, *J. Am. Ceram. Sci.* **65** (1982) 284.
7. R. H. DAUSKARDT, D. K. VEIR and R. D. RITCHIE, *ibid.* **72** (1989) 1124.
8. B. N. COX, D. B. MARSHALL, D. K. KOURIS and T. MURA, *J. Eng. Mater. Technol.* **110** (1988) 105.
9. L. R. F. ROSE and M. V. SWAIN, *Acta Metall.* **36** (1988) 955.
10. C. S. YU and D. K. SHETTY, *J. Am. Ceram. Sci.* **72** (1989) 921.
11. R. C. GARVIE, R. H. J. HANNINK and M. V. SWAIN, *J. Mater. Sci. Lett.* **1** (1982) 437.
12. A. H. HEUER, *J. Am. Ceram. Sci.* **70** (1987) 689.
13. D. POST, in "Handbook on Experimental Mechanics", edited by A. S. Kobayashi, (Prentice-Hall, Englewood Cliffs, New York, 1987) Ch. 7.
14. X. L. QING, F. L. DAI and Y. W. QIN, *Opt. Las. Eng.*, in press.
15. F. L. DAI, J. MCKELVIE and D. POST, *ibid.* **12** (1990) 101.
16. D. S. DUGDALE, *J. Mech. Phys. Solids* **8** (1960) 100.

Received 12 October 1994
and accepted 28 April 1995